



Supplement of

Damage functions for climate-related hazards: unification and uncertainty analysis

B. F. Prah1 et al.

Correspondence to: B. F. Prah1 (corr@prahl.net)

The copyright of individual parts of the supplement might differ from the CC-BY 3.0 licence.

1 Supplementary information for the Lisbon case study

For the Lisbon case study, we combine orographic, land-cover, and socio-demographic data. The Lisbon urban cluster was obtained from Zhou et al. (2013), who employed a clustering algorithm to CORINE land-cover data. Figure 1 shows the extent of the urban cluster. It includes several connected suburbs along the shores of river Tejo and the north of the Setúbal peninsula.

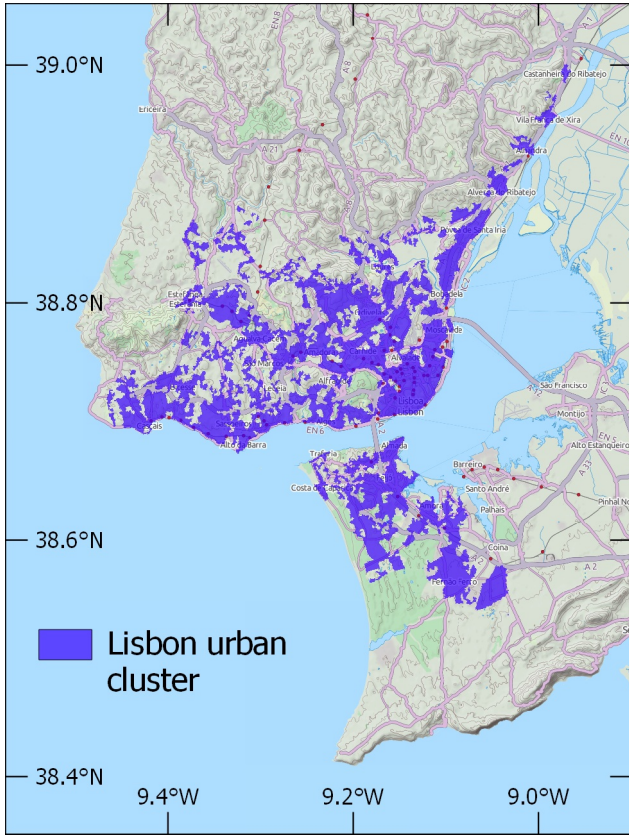


Figure 1. The Lisbon urban cluster as supplied by Zhou et al. (2013). The blue-shaded areas are classified as continuous and discontinuous urban fabric (CORINE landcover classes I and II).

Table 1. The incremental and total number of flooded buildings within the Lisbon urban cluster at flood levels between 0 and 10 m

Flood level [m]	Flooded buildings	
	Increment	Total
0.0	0	0
0.5	19	19
1.0	9	28
1.5	8	36
2.0	7	43
2.5	24	67
3.0	40	107
3.5	39	146
4.0	64	210
4.5	243	453
5.0	217	670
5.5	218	888
6.0	396	1284
6.5	337	1621
7.0	274	1895
7.5	461	2356
8.0	303	2659
8.5	366	3025
9.0	410	3435
9.5	550	3985
10.0	493	4478

Table 1 shows the number of flooded buildings within the Lisbon urban cluster at flood levels up to 10 m. These were obtained by downscaling of statistical data provided by the Instituto Nacional de Estatística¹ via 2006 CORINE land-cover data. Inundated areas were determined from the EU-DEM², a hybrid digital elevation model based mainly on SRTM and ASTER GDEM data.

¹ <http://www.ine.pt>

² <http://www.eea.europa.eu/data-and-maps/data/eu-dem>

2 Variance-based sensitivity analysis

2.1 Method

We conduct a variance-based sensitivity analysis following the approach outlined in Saltelli et al. (2008).

First, we generate two $(n \times d)$ matrices \mathbf{A} and \mathbf{B} , where each column represents one of d input vectors of size n . The matrices are filled with uniformly distributed random values between 0 and 1. We use the inverse cumulative distribution function (ICDF) to convert the input vectors to the respective dependent random variables of the damage model. For input vector i , we construct matrix $\mathbf{C}_{(i)}$ such that we take all columns $j \neq i$ from \mathbf{A} and column $j = i$ from \mathbf{B} . Using the recommended Jansen estimator (Saltelli et al., 2010) to evaluate the total-effects index TE_i of our damage model $f(\cdot)$, we write

$$\text{TE}_i = \frac{\frac{1}{2n} \sum_{l=1}^n \left(f(\mathbf{A})_l - f(\mathbf{C}_{(i)})_l \right)^2}{\text{Var}(Y)}, \quad (1)$$

with

$$\text{Var}(Y) = \frac{1}{2n} \sum_{l=1}^n \left(f(\mathbf{A})_l^2 + f(\mathbf{B})_l^2 \right) - \left(\frac{1}{n} \sum_{l=1}^n f(\mathbf{A})_l + f(\mathbf{B})_l \right)^2. \quad (2)$$

In Eq. (2), we include both matrices \mathbf{A} and \mathbf{B} in order to obtain a closer estimate of the model's variance than by using matrix \mathbf{A} alone.

For the estimation of the first-order effect FO_i we do not employ the estimator recommended by Saltelli et al. (2010), which appears to be robust only for variables with zero mean. Instead, we use the corresponding Jansen estimator (Jansen, 1999; Saltelli et al., 2010) whose results rapidly converge with increasing sample size n . Hence, the first-order effects index FO_i is given by

$$\text{FO}_i = 1 - \frac{\frac{1}{2n} \sum_{l=1}^n \left(f(\mathbf{B})_l - f(\mathbf{C}_{(i)})_l \right)^2}{\text{Var}(Y)} \quad (3)$$

The extension to higher-order interactions is straightforward. For second-order interactions, we construct matrix $\mathbf{C}_{(i,j)}$ such that we take all columns $l \notin \{i, j\}$ from \mathbf{A} and all columns $l \in \{i, j\}$ from \mathbf{B} . To estimate the second-order effect $\text{SO}_{i,j}$, we replace $\mathbf{C}_{(i)}$ with $\mathbf{C}_{(i,j)}$ in Eq. (3) and subtract first-order effects of input variables i and j . It fol-

lows that

$$\text{SO}_{i,j} = 1 - \frac{\frac{1}{2n} \sum_{l=1}^n \left(f(\mathbf{B})_l - f(\mathbf{C}_{(i,j)})_l \right)^2}{\text{Var}(Y)} - \text{FO}_i - \text{FO}_j \quad (4)$$

for $i \neq j$.

Similarly, we calculate the third-order effect $\text{TO}_{i,j,k}$ by constructing the corresponding matrix $\mathbf{C}_{(i,j,k)}$ and subtracting lower-order terms,

$$\text{TO}_{i,j,k} = 1 - \frac{\frac{1}{2n} \sum_{l=1}^n \left(f(\mathbf{B})_l - f(\mathbf{C}_{(i,j,k)})_l \right)^2}{\text{Var}(Y)} - \text{FO}_i - \text{FO}_j - \text{FO}_k - \text{SO}_{i,j} - \text{SO}_{i,k} - \text{SO}_{j,k} \quad (5)$$

for $i \neq j \neq k \neq i$.

It is clear from inspection, that Eqs. (4) and (5) simplify considerably for models with only two and three random variables, respectively. For models with only two random variables, the second-order index becomes

$$\text{SO}_{1,2} = 1 - \text{FO}_1 - \text{FO}_2. \quad (6)$$

Similarly, for models with three random variables the third-order index simplifies to

$$\text{TO}_{1,2,3} = 1 - \text{FO}_1 - \text{FO}_2 - \text{FO}_3 - \text{SO}_{1,2} - \text{SO}_{1,3} - \text{SO}_{2,3}. \quad (7)$$

2.2 Additional results

Figure 2 shows the first-, second-, and third-order effect indices for the intrinsic uncertainties in both the microscale and the macroscale damage function. If compared with the total-effects index (cf. Fig. 5 of the main paper), it is seen that the first-order effects are the dominant contribution to the total effects index. Panels (c) and (d) show that there is some interaction between the variation in asset value and the uncertainty of the threshold exceedance. However, this interaction is limited to inundation levels below 1 m and only contributes lightly to the overall model variance (less than 0.2 of output variance). Figure 2 also shows that third-order effects are negligible.

A similar picture arises for the second-order interaction between intrinsic and extrinsic (hazard threshold) uncertainties within the macroscale damage function (Fig. 3). The interaction seen for flood levels below 0.5 m is due to the fact that the uncertainty in the hazard threshold determines the occurrence of a damage at such low flood levels and that, consequently, the intrinsic uncertainties are contingent on the occurrence of a damaging event.

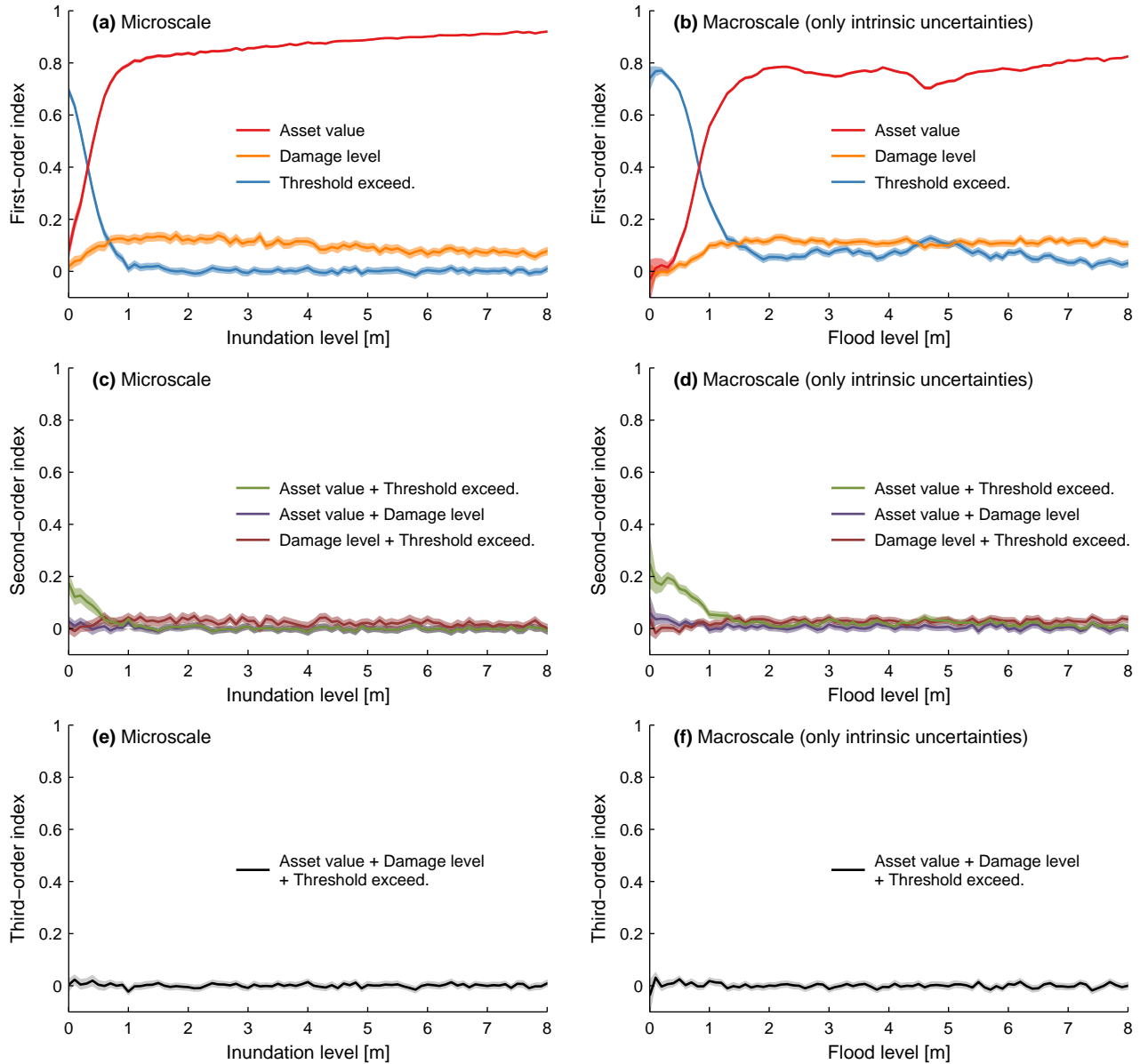


Figure 2. Results of the sensitivity analysis of the microscale (**a, c, and e**) and the macroscale (**b, d, and f**) damage function, taking into account only intrinsic uncertainties. Each column comprises the first-, second-, and third-order effects of the respective uncertainty source on the output variance. First order effects are directly attributable to a source of uncertainty, while higher-order effects arise from interactions between two or more uncertain variables.

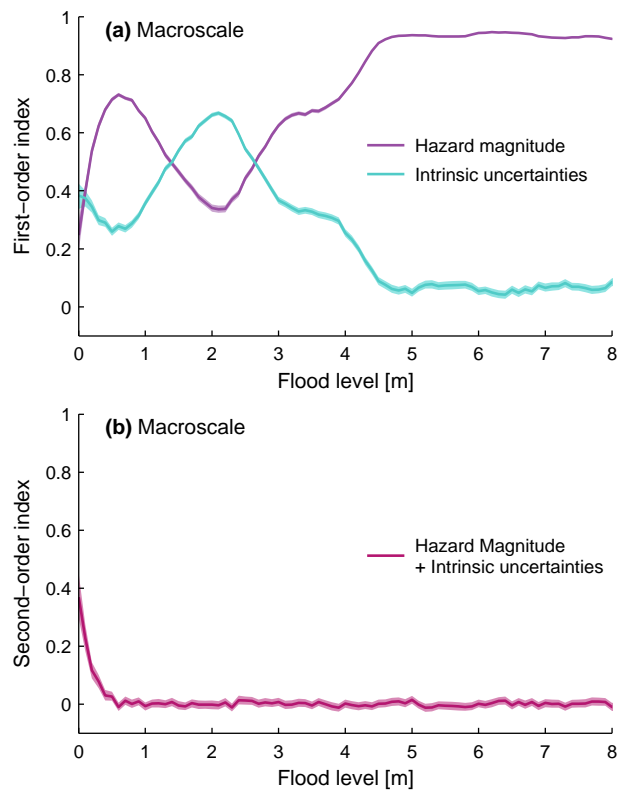


Figure 3. Results of the sensitivity analysis of the macroscale damage function, relating the joint effect of intrinsic uncertainties on the output variance to the effect of uncertainty in the hazard threshold. Panel (a) shows the direct, first-order effect, while panel (b) shows the second-order effect due to interaction between the uncertainty sources.

References

- Jansen, M. J.: Analysis of variance designs for model output, *Comput. Phys. Commun.*, 117, 35 – 43, doi:10.1016/S0010-4655(98)00154-4, 1999.
- Saltelli, A., Ratto, M., Andres, T., Campolongo, F., Cariboni, J., Gatelli, D., Saisana, M., and Tarantola, S.: *Global Sensitivity Analysis. The Primer*, John Wiley & Sons, 2008.
- Saltelli, A., Annoni, P., Azzini, I., Campolongo, F., Ratto, M., and Tarantola, S.: Variance based sensitivity analysis of model output. Design and estimator for the total sensitivity index, *Comput. Phys. Commun.*, 181, 259 – 270, doi:10.1016/j.cpc.2009.09.018, 2010.
- Zhou, B., Rybski, D., and Kropp, J. P.: On the statistics of urban heat island intensity, *Geophysical Research Letters*, 40, 5486–5491, doi:10.1002/2013GL057320, 2013.